

Article

# QSI Methods for Determining the Quality of the Surface Finish of Concrete

Francisco Javier Benito Saorin <sup>1,\*</sup>, Isabel Miñano Belmonte <sup>1</sup>, Carlos Parra Costa <sup>1</sup>,  
Carlos Rodriguez Lopez <sup>2</sup> and Manuel Valcuende Paya <sup>3</sup>

<sup>1</sup> Department of Architecture and Building Technology, Technical University of Cartagena, Paseo Alfonso XIII, 30203 Cartagena, Spain; isabelminano@hotmail.es (I.M.B.); Carlos.parra@upct.es (C.P.C.)

<sup>2</sup> Department of Construction Material, Technological Research Center of Murcia Country, 30820 Alcantarilla, Spain; crodriguez@ctcon-rm.com

<sup>3</sup> Department of Architecture Constructions, Polytechnic University of Valencia, Camí de Vera, 46022 Valencia, Spain; mvalcuen@csa.upv.es

\* Correspondence: franciscojavierbenito@hotmail.es; Tel.: +34-868-07-1250

Received: 1 March 2018; Accepted: 21 March 2018; Published: 23 March 2018



**Abstract:** The surface finish of a concrete element may become an index of its quality, relating the external and internal porosity with the mechanical and durability properties. Few methods are used to determine the surface quality of concrete elements. Mention must be made the Quality Surface Index (QSI) proposes a simplified method to quantify the surface occupied by the pores in relation with the total surface inspected, analyzing groups of pores by their diameter. The method of the CIB W29 (Commission W29 “Concrete Surface Finishings”) proposes an inspection of the concrete element and its visual comparison with some standard templates. Finally, the digital processing of images allows the zones with surface defects to be delimited and quantified according to premises of quality introduced into the control software. These three methods are employed in this work and are applied in three concrete walls situated three meters from the observer (M-1, M-2 and M-3). Following the conversion of the results of the method with ImageJ and QSI, the results suppose differences that go from 0.1 tenths (2%) for M-3 up to 0.3 tenths (8%) for M-1. All values are within the obtained range with CIB W29 templates. This can validate the QSI and digital processing methods and allows a quick verification of the results. With the digital method, it is obtained that 23.5% of the total pores of M-1 have a diameter of less than 10 mm<sup>2</sup> and 44% of less than 100 mm<sup>2</sup>. For M-2 and M-3 the proportions of pores with a dimension below 10 mm<sup>2</sup> is of 43.1% and 27.7%, respectively, and that 77.5% and 60.7% are smaller than 100 mm<sup>2</sup>. From all the above it can be highlighted that M-1 is the one with the lowest amount of pores, however the proportion of the largest is greater than for M-2 and M-3. In the case of M-3, although it has a lower proportion of larger pores than M-1, its greater amount means it is the worst in terms of surface finish of the three.

**Keywords:** surface finish; pores; bubbles and analysis of images

## 1. Introduction

A good surface finish should be demanded of concrete elements, especially for architectonic concretes that are not to be coated. There are several investigations [1–10], that developed methods of visual inspection and non-destructive tests. None of them, except the QSI method [3], is a simple method to be used in the work by a non-specialist operator.

The surface finish of a concrete element may become an index of its quality, relating the external and internal porosity with the mechanical properties and durability. Surface pores are the result of not having liberated some of the air bubbles present in the concrete in contact with the formwork.

The amount of occluded air in the concretes is influenced principally by the dosage, the granulometry of the aggregates, the type of mixing, the height of the pouring, and the type of formwork [11]. High viscosity limits the evacuation of the occluded air [12].

The increase in surface pores can mean a reduction in the durability of the concrete. Moreover, higher surface porous promotes the accumulation of contaminant agents or the colonization of microorganism that act in detriment of its aesthetic appearance, and even in the durability of the concrete [13]. Likewise, the water that can be retained in these surface pores accelerates possible chemical, sulphate, or chloride attacks. Together with all this, the greater surface of concrete in contact with the exterior, as well as the depth of the surface pores themselves, can produce an increase in the depth of the carbonation front [14]. Therefore, reducing the surface porosity of concrete can improve its durability and increase its useful life, reducing its ecological impact (more sustainable).

There are few methods that are used to determine the surface quality of concrete elements. Mention must be made the QSI [3] method proposes a simplified method to quantify the surface occupied by the pores in relation with the total surface inspected, analyzing groups of pores by their diameter. The three main advantages of the QSI method, with respect to other methods of the literature [4,8,15], is its simplicity in determining and quantifying the surface quality of concrete; it does not require high knowledge in digital processing, can be applied on curved surfaces, and even with different shades or surface spots. The QSI method can simplify quality control of surface finish in architectural concrete. It is suitable for inspections in small areas (statistical control). The method is less suitable for large inspection areas, due to the increase in work. In other areas of construction, there are investigations that could be used in the surface finish of the concrete [10].

With other methods studied [1,2,4–10] it is not possible to quantify the quality of the surface finish of concrete elements in a simple way on the construction site and by non-specialized workers. Majchrowski et al. [8] use an advanced three-dimensional (3D) scanner (topographic analysis) to analyze concrete surfaces.

One of the simplest methods found, although it does not quantify, is the method of the CIB W29; it proposes an inspection of the concrete element and its visual comparison with some standard templates. The method includes two steps to carry out (Figure 1): a visual comparison and obtaining results. It is not an objective method and depends on the skill of the technician who carries them out, making it difficult for another observer to repeat the criteria.

The digital processing of images [4,10,15] allows the zones with surface defects to be delimited and quantified according to premises of quality introduced into the control software. This method eliminates the subjectivity of the results [4], but introduces variables that must be analyzed correctly to obtain results that correspond to the reality. These variables can vary for each concrete element (luminosity, roughness, geometry, etc.). To digitally process images, a minimum of five steps are required (Figure 1) and some of them can be repeated on several occasions until the desired results are obtained (trial and error). The inspection, and above all, the analysis of the results requires technical decisions, especially in heterogeneous material such as concrete, requiring a technical control to take decisions of adjustment in the analysis program, such as in the color balance, contours, cavities, regions, circularity index, adjustment of shades, or even the detection of anomalies within blemishes, above all in large-sized pores where the semi-spherical form is lost and their digital analysis becomes difficult. The automation of cataloguing the surface finish with image processing shows itself to be adequate for tasks requiring great accuracy, permitting the analysis of very small pores and in large amounts. The digital method can analyze large wall surfaces if the quality of the images allows it. This method must be simplified to achieve good results in a simple way. For all this, work should be done to achieve a simple and standardized work protocol to simplify the quality control of the surface finish of concrete elements, including simplifying the inspection from a mobile phone application. All this could facilitates the communication between architects, engineers, contractors, and concrete manufacturers when seeking to define a surface finish in architectural concrete.

The present work goes deeper into the digital analysis of images with the program ImageJ [16], as an indicator of the surface quality of concrete elements. Moreover, it shows and compares this with two other inspection methodologies: the manual QSI method and the method proposed in the CIB W29. It becomes clear that it is necessary to elaborate standardized methodology that permits the quantification of the quality of architectural concretes [17].

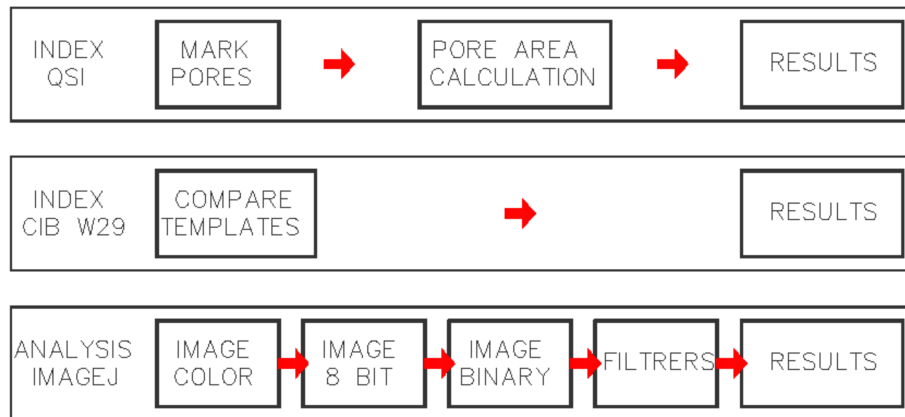


**Figure 1.** Operational scheme of each system.

## 2. Methods

A scheme of the steps to follow in the three methods used is shown in Figure 1. The results of the experimental work and the comparison of results among the three methods allow the checking of the efficacy of the digital analysis of images and the advantages of each method.

### 2.1. QSI Method

The denominated QSI method consists in quantifying the surface occupied by the pores in relation with the total surface inspected. The first step of the method is to identify the size of each pore and the second is to add up its surfaces. To do so, in general, five groups of pores are formed according to diameter (2, 4, 6, 8, and 10 mm). To include the pores in one of the groups, it must be possible to inscribe it in the circumference of diameter of each group chosen and not belong to a smaller group (Figure 2). When a pore or air pocket has a diameter greater than 10 mm it is decomposed into several of smaller diameter. All this enables greater simplification of the working methodology, and the ability to carry out a manual data gathering with a subsequent mathematical and statistical analysis with a simple easily handled spreadsheet. Depending on the precision of the results and the visibility of the concrete (location of the element), the five groups of pores indicated can be used or some can be discarded. The method is effective on irregular surfaces.

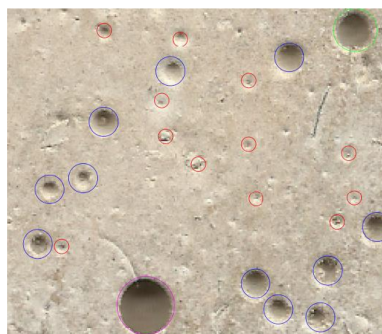


**Figure 2.** Scheme and example of data collection with the Quality Surface Index (QSI) method.

## 2.2. CIB W29 Method

In 1971, the working group W29 of the CIB established a scale to classify concretes by their degree of surface quality, with values from 1 to 7 (from lesser to greater amount of surface damage). The scale has seven images of concretes used as templates (Figure 3), with different amounts of surface pores that can be compared visually with the concrete element. The CIB W29 indicates that the surface quality of the concrete can be considered high if at a distance of 3 m the blemishes of the concrete cannot be visually discerned. If the distance must be increased to 4 m, the quality descends to good. At 5 m the surface quality of the concrete is considered normal. If a greater distance is required to be unable to appreciate a damaged zone in the element, the surface finish is not good.

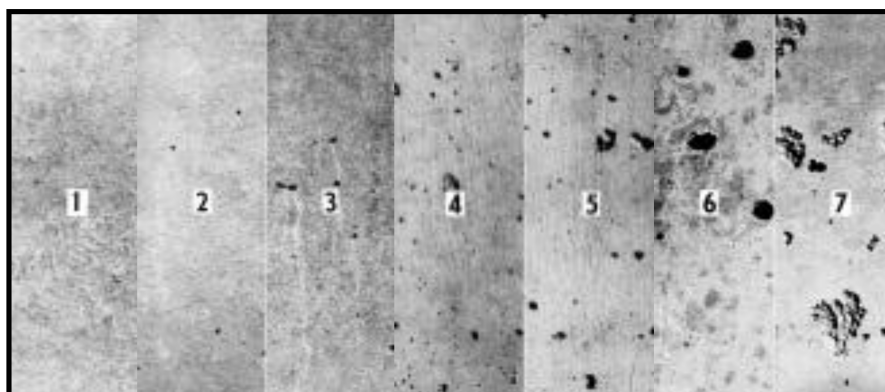


Figure 3. Templates of surface quality, from 1 to 7, according to CIB W29.

## 2.3. Digital Method

The method of digital analysis using the program ImageJ can provide quantitative information on the quality of the surfaces of concrete. ImageJ is a program to process and analyze images.

After delimiting the zone of inspection, the images of concrete to inspect were imported into the program ImageJ. The image was converted to 8 bit black and white (binarization) to highlight the surface blemishes (Figure 4), and to avoid changes in tone or stains in the concrete from affecting the results. Additionally, the color was balanced in tones of black and white. The image was scaled and adjusted to the equivalence between the pixels of the image and the known dimensions of the inspection. Different filters of size and shape of the pores to be analyzed were applied, and the areas of each of them were calculated and displayed. If the results obtained were optimal for the requirements of the investigation, then the inspection was ended. If on the other hand, errors were detected in the analysis due to poor adjustment of the filters or color balance the process was repeated until the optimal results are obtained (trial and error). The size of the pore analyzed must be adjusted according to the requirements of the analysis.

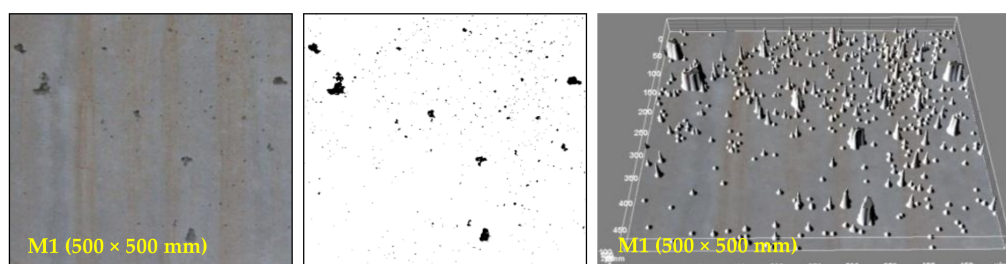
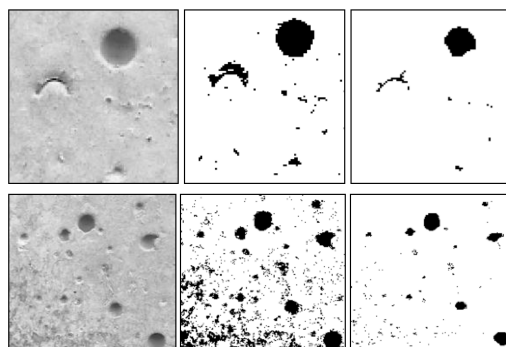


Figure 4. From left to right: zone analyzed, image in black and white and representation of results.



The suitability of the adjustments in ImageJ must be determined according to the results obtained and the precision required. If the surface of the concrete is curved, or has shadows of different intensity on the zone analyzed, by different light sources or large pores, the analysis of the surface pores becomes more difficult and requires several adjustments to minimize the effects of the non-homogeneous shadows [15]. The adjustments in the color balance of the images affect the final results by a modification in the size of the pores (Figure 5).



**Figure 5.** Top and bottom, examples of differences in the adjustment of the color balance that affect the results.

Also, the analysis with ImageJ permits another type of analysis, such as the index of circularity (I-C). This index allows the analysis, or even filtering, of the results, depending on the more or less regular shape of the pores. With a value of 100%, the pores are totally circular, and with the decrease in this, the shapes of the pores become irregular.

### 3. Objectives and Experimental Program

The three methods were applied in three concrete walls situated three meters from the observer (Figure 6).



**Figure 6.** Three concrete walls analyzed (M-1, M-2 and M-3, from left to right).

#### 3.1. Surface Finish Determination with the QSI Method

In this work, the pores of more than 4 mm in diameter are analyzed in the QSI method. The number of pores of each group in the inspected area is counted (Figure 2) and the proportion of the surface of them all were calculated with respect to the 100% of the inspected zone with the following expression:

$$QSI(\%) = \frac{Blemished\ surface \times 100}{inspected\ area\ (500 \times 500\ mm)} \quad (1)$$

where,

$$Blemished\ surface = n^{\circ}B_{10} \times AB_{10} + n^{\circ}B_8 \times AB_8 + n^{\circ}B_6 \times AB_6$$

$n^{\circ}B_n$ , is the number of pores detected for the different diameters, in this case “n” is 10, 8, and 6 mm.

$AB_n$ , is the area of the pore idealized as circles 10, 8, and 6 mm in diameter. Those values are constant for the different calculations.

### 3.2. Surface Finish Determination with Digital Method

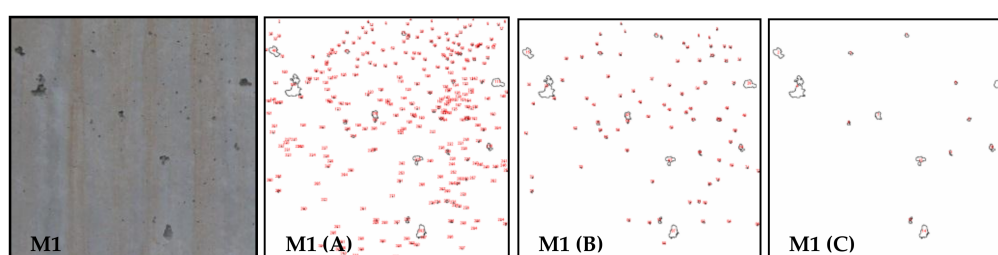
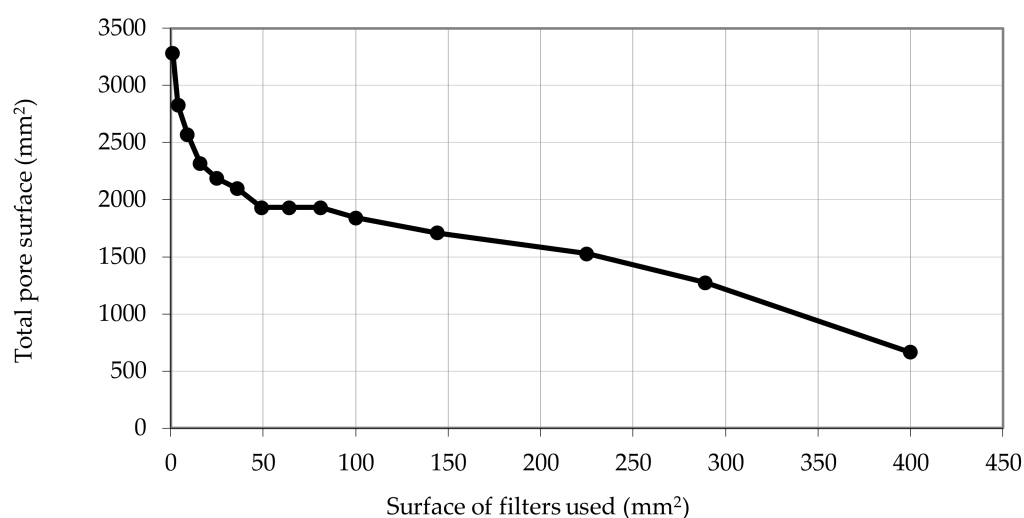
The results of the processing and digital analysis of images they are linked with the quality of the images used. In this work, a Canon digital camera of 10 megapixels was used situated perpendicularly, with indirect natural light to avoid alterations in the shadows generated in the interior of the pores of the parameters of concrete analyzed. The image calibration was carried out placing a measuring pattern on the element observed, which enabled the equivalence between the pixels of the image and the real dimension to be obtained.

On the other hand, the images must be binary for an adequate analysis. The ImageJ program allows conversion of a color image into an 8-bit binary image. This consists of a process of reducing the information of the same, in which only two values persist: 0 and 1, or the colors black and white, as in this case.

The total number of pores, their size, and the percentage of the concrete surface that they occupy are the principal parameters that affect the perception of surface quality of concrete elements and the proportion of which can be obtained with the program ImageJ. For the same percentage of surface with pores, the increase in the amount of these implies a smaller size, which at a certain distance could mean that the pores are imperceptible. However, with the same percentage but with a smaller amount of pores, they could be visible from a greater distance, due to their greater size. Therefore, the amount of pores, the percentage of surface affected by these pores, and the distance from which the concrete element will be visualized must be analyzed [15]. The demands of surface quality on a wall in a transited zone must be far greater than those of a wall in a remote site. For the former, the filters must be more precise, with analysis of pores of a much smaller size than for the latter wall. The size of the pores filtered has an important impact on the final results. In the real case of this experimental work, in the prior calibration work, and as an example to explain the measurement process with the different filters, in the wall M-1 (Figure 6) inspected with the filter of  $1 \times 1$  (the size of the pores taken into account is greater than  $1 \text{ mm}^2$ ), 312 pores were found, occupying 1.31% of the inspection surface ( $500 \times 500 \text{ mm}$ ). When the filter was increased to  $5 \times 5$ ,  $10 \times 10$  or  $20 \times 20$ , the amount of pores descends to 25, 6, and 1, and the surface area affected descended to 0.87%, 0.74% and 0.27%, respectively (Table 1). The results of the filters used are shown in Figure 7. A profile of the typology of surface pores detected in M-1 is represented according to the filter used. With the  $1 \text{ mm}^2$  ( $1 \times 1$ ) filter, 312 pores were obtained with a total surface affected of  $3285 \text{ mm}^2$ ; however, with the filter of  $400 \text{ mm}^2$  ( $20 \times 20$ ) only one pore is obtained of  $664 \text{ mm}^2$ . This profile can determine the suitability of each filter depending on the demands of the investigation and the inspection distance (Figure 8). With the results obtained, five filters were created, grouping them by their level of precision (A, B, C, D, or E). Thus for example, the type A filters (Figure 8 and Table 1) could be optimal for works where a great deal of precision is required in the results, with the analysis of pores of up to  $1 \text{ mm}$ . The B type filters could be appropriate for precision works where the inspection distance is somewhat greater than in the type A, which renders pores of  $1 \text{ mm}^2$  imperceptible. The type C and D filters are appropriate for inspections on walls that are not visible at a short distance, and finally those of type E which only provide information of large pores or air pockets, the most visible at middle distances. Filters greater than  $20 \times 20$  could be used in special works, although zones of pores larger than  $400 \text{ mm}^2$  could significantly alter the mechanical properties of the concrete, requiring, as well as aesthetic analysis, a study of the mechanical properties of the zone.

**Table 1.** Results of M-1 with different filters in ImageJ.

(X-Y)	Sup. Filter (mm <sup>2</sup> )	N° Pores	Total Area of Area mm <sup>2</sup>	% Area	Type of Filter
1 × 1	1	312	3285	1.3%	A
2 × 2	4	88	2826	1.1%	B
3 × 3	9	42	2572	1.0%	B
4 × 4	16	21	2316	0.9%	B
5 × 5	25	14	2185	0.9%	C
6 × 6	36	11	2096	0.9%	C
7 × 7	49	7	1930	0.8%	D
8 × 8	64	7	1930	0.8%	D
9 × 9	81	7	1930	0.8%	D
10 × 10	100	6	1840	0.7%	D
12 × 12	144	5	1709	0.7%	D
15 × 15	225	4	1528	0.6%	D
17 × 17	289	3	1274	0.5%	E
20 × 20	400	1	664	0.3%	E

**Figure 7.** From left to right: Image of M-1 and results with filters 1 × 1 (A), 2 × 2 (B) and 5 × 5 (C).**Figure 8.** Total surface of pores depending on the filter used on M-1.

### 3.3. Conversion of Percentage Values to the CIB Scale

With the objective of validating the results obtained with the QSI method and with the digital analysis, the percentage results obtained with both methods are transformed to the scale of 1 to 7 proposed and used by CIB W29. To do so, previously the templates proposed by CIB W29 are analyzed with both methods, following the procedure described in the previous sections. Given the singularity of the templates (Figure 9) in the QSI method, a surface damage greater than 10 mm in diameter was been added, delimiting its real contour (orange in the Figure 9). Additionally, the pores of 2 mm were not been considered, due to the difficulty entailed in carrying out the inspection with the low resolution templates. With the results obtained, a conversion or equivalence of the values catalogued

by the CIB (from 1 to 7) was posed and for those obtained with the QSI method. To do so, a relation is made between both series of data and the expression that best fit was obtained among both series of data, in this case  $Y = 1.69\ln(x) + 9.99$ , which fit the data used, to 98% (Figure 10).

The values in the 1 to 7 scale with one decimal, were obtained introducing the percentage results of the QSI method as “x” in the expression. This transformation allows maintaining the use of the scale and validating the results obtained. In a similar manner, the conversion of the percentage results of the digital analysis at the scale of 1 to 7 was carried out. For this, on each one of the templates proposed by the CIB W29, the inspection using ImageJ was carried out. In Figure 11, the analysis with ImageJ of the templates 4, 6 and 7 of the CIB W29 code is shown as an example. In this case, the expression  $Y = 0.99\ln(x) + 8.67$  fits the data used to 99% (Figure 10).

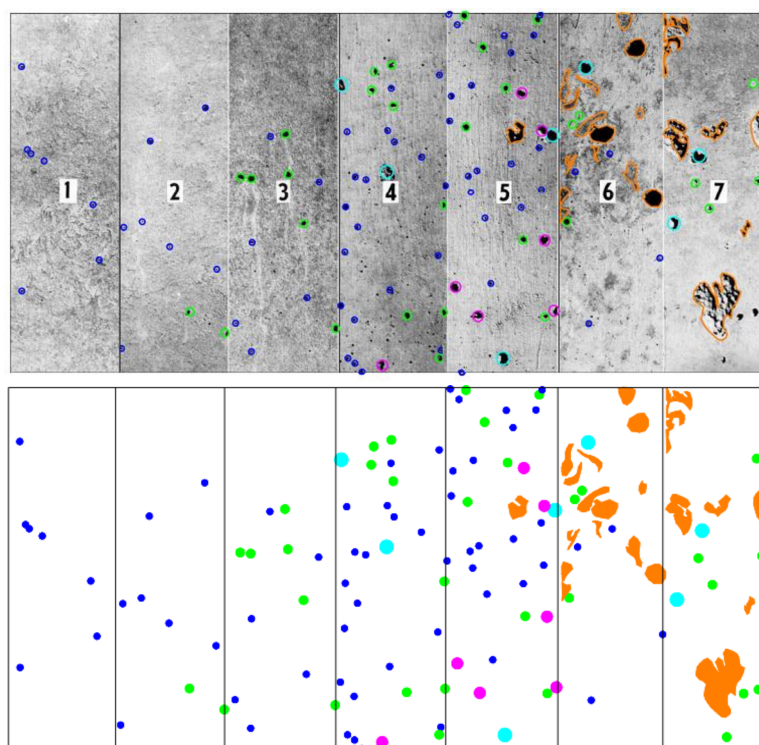


Figure 9. Application of the QSI method and ImageJ on the templates of the CIB W29 code.

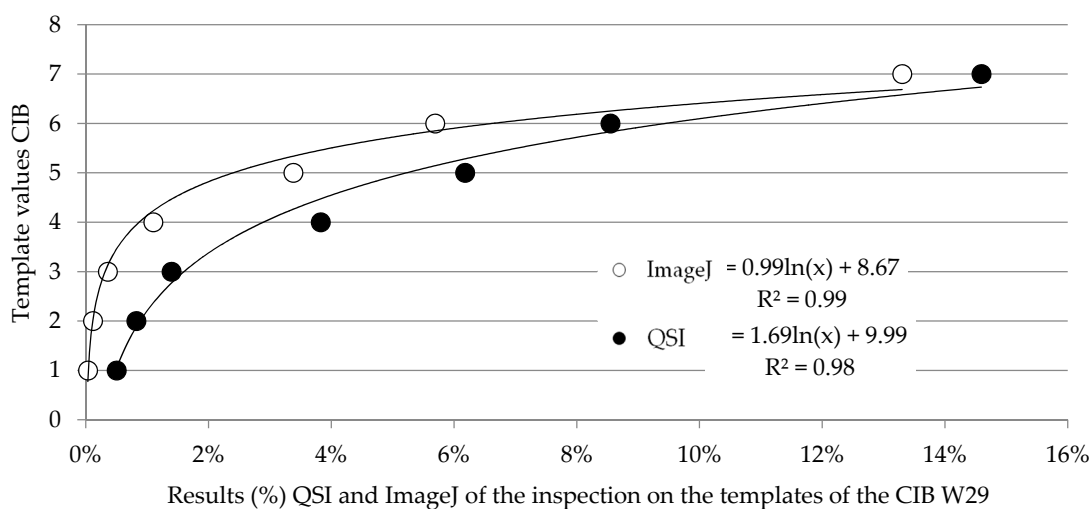


Figure 10. Relation of the templates of CIB W29 and values for QSI and ImageJ.

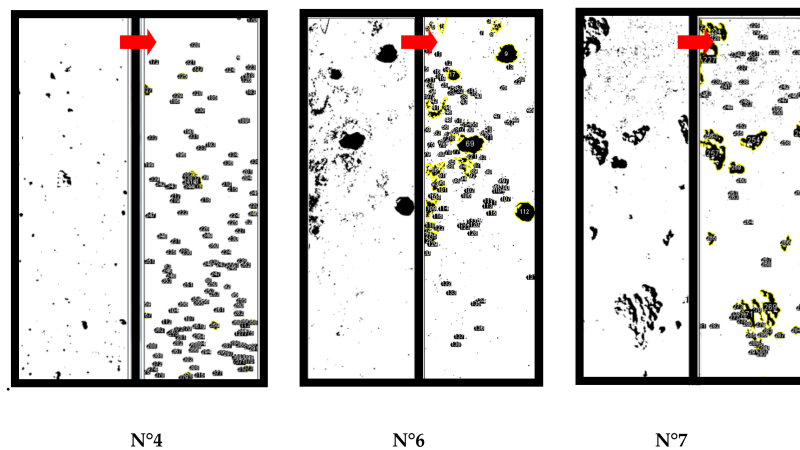


Figure 11. Analysis with ImageJ of templates 4, 6, and 7 of the CIB W29 code.

The results of the analysis with ImageJ of the seven templates of the CIB are shown in Figure 12. From them, it can be highlighted that with the increase in the value of the templates, the amounts of porosity and size increase. With ImageJ, the large pores or air pockets are not correctly analyzed according to their real contour without decomposition into several contours, leaving zones without being included.

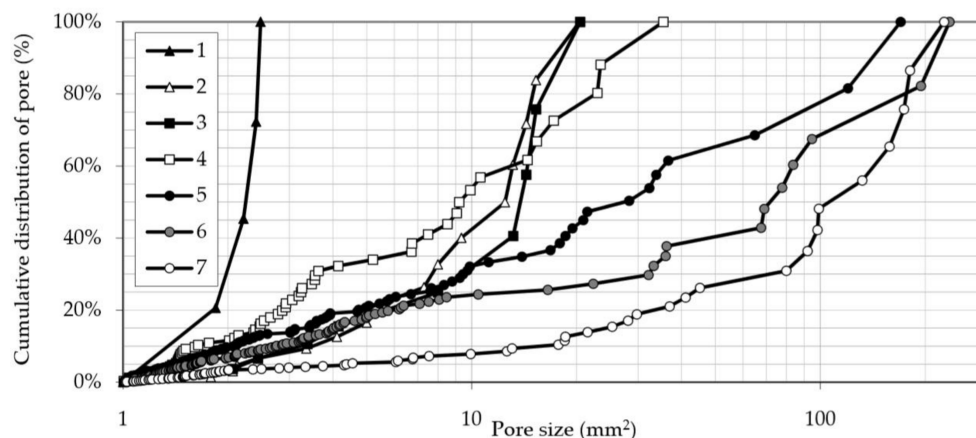


Figure 12. Result of the analysis with ImageJ of the 7 templates of the CIB W29.

#### 4. Results and Discussion

The analysis of the surface quality of three concrete walls was carried out with ImageJ, the QSI method and with CIB W29 templates. The inspection area of 250,000 mm<sup>2</sup> (500 × 500 mm) was determined.

##### 4.1. QSI Method

On inspection zones, the QSI method was applied, counting the pores larger than 4 mm (Figure 13) and grouping them according to their diameters. In Figure 14, the accumulated results of the surface porosity for each wall are shown, with the greater porosity of M-3 (7059 mm<sup>2</sup>) standing out, against the similar results for M-1 and M2 (3716 and 3556 mm<sup>2</sup>, respectively). For the case of M-1, the calculations of the area are:

$$\text{Area}_{M1} = n^{\circ}B_{10} \times AB_{10} + n^{\circ}B_8 \times AB_8 + n^{\circ}B_6 \times AB_6 = 25 \times 78.54 + 9 \times 50.26 + 46 \times 28.27 = 3716 \text{ mm}^2$$



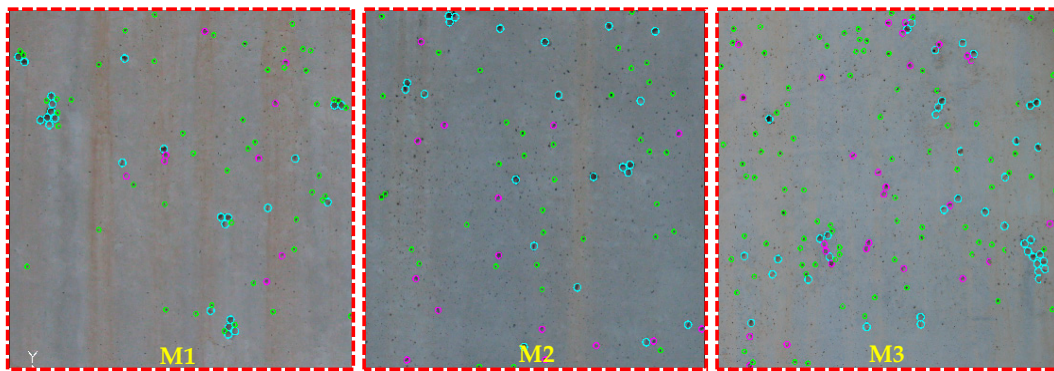


Figure 13. Inspection carried out with the QSI method on M-1, M-2 and M-3 (from left to right).

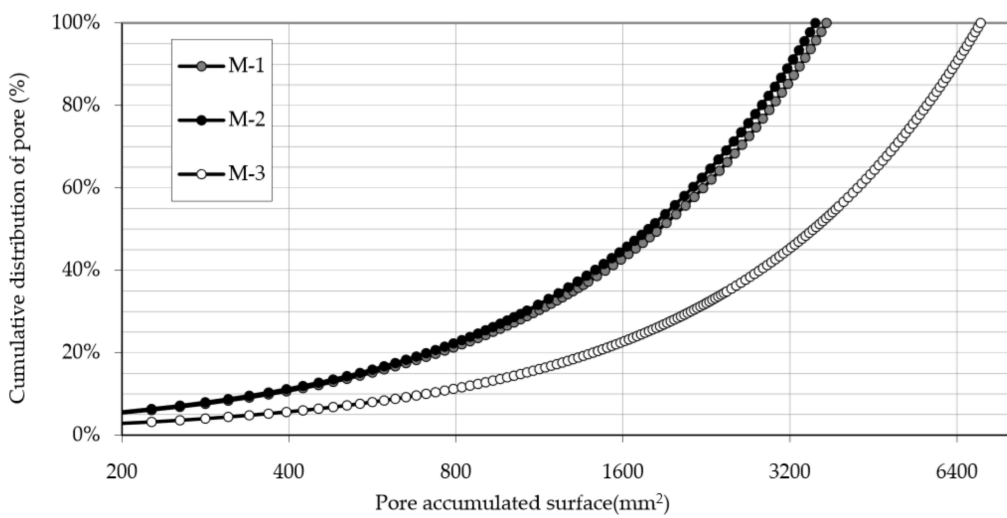


Figure 14. Result of the QSI method for M-1, M-2 and M-3.

4.2. CIB W29 Method

In Figure 15, the three delimited zones are shown. Together with the marked zone, the seven templates of the CIB W29 are shown for visual comparison. The template that most resembles the inspection zone was sought. The numerical results are shown in Table 3.

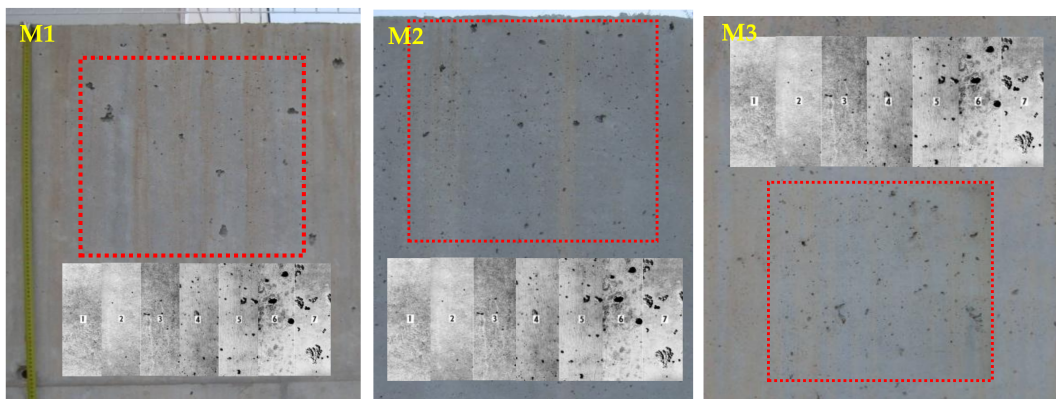


Figure 15. Inspection done with the CIB method on M-1, M-2 and M-3 (from left to right).

### 4.3. Digital Method

A detailed analysis of some zones of the walls was carried out with ImageJ, with a prior work of calibration and choice of the filter used (Section 3.2). It was adopted that the pore size taken into account was greater than  $1 \text{ mm}^2$  (the  $1 \times 1$  filter). With larger filters, such as  $5 \times 5$ ,  $10 \times 10$  or  $20 \times 20$ , the amount of detected pores decreased, and the affected surface decreases significantly.

Figure 16 shows a representation of the results of M-1. The cumulative percentage distribution of the size of pores of each of the walls inspected is shown in Figure 17 with the  $1 \times 1$  filter, which was the most precise used in this work. From the results represented in Figure 17, the 23.5% of the total pores of M-1 had a diameter of less than  $10 \text{ mm}^2$ , and 44% of less than  $100 \text{ mm}^2$ . For M-2 and M-3, the proportions of pores with a dimension below  $10 \text{ mm}^2$  were of 43.1% and 27.7%, respectively and that 77.5% and 60.7% are smaller than  $100 \text{ mm}^2$ . From all of the above, it can be highlighted that M-1 was the one with the lowest amount of pores; however, the proportion of the largest is greater than for M-2 and M-3. In the case of M-3, although it had a lower proportion of larger pores than M-1, its greater amount meant that it was the worst in terms of surface finish of the three, as is reflected in Table 2. Also, M-3 was the wall that obtained the lowest index of circularity (Table 2), due, principally to the grouping of several pores.

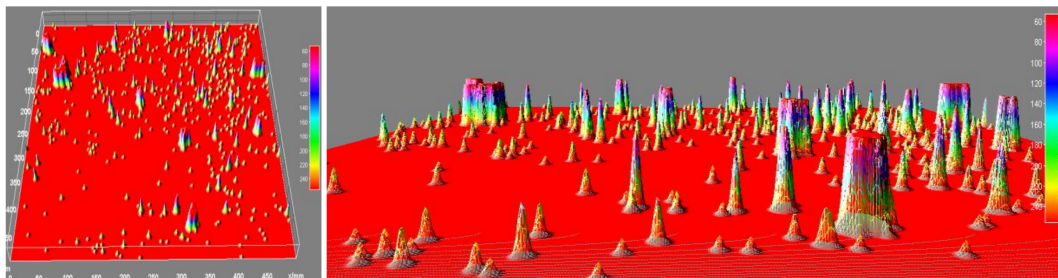


Figure 16. Representation of the results of M-1 with ImageJ.

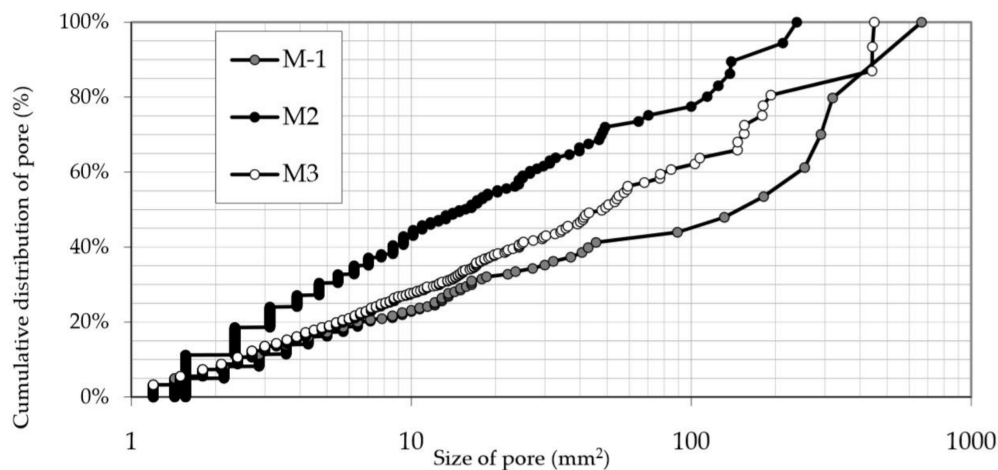


Figure 17. Cumulative distribution of pore M-1, M-2 and M-3 with ImageJ.

Table 2. Summary of results of the analysis of images with ImageJ of M-1, M-2 and M-3.

	N° Pores	Total Area $\text{mm}^2$	% Area	Index Circ. (I-C)
M-1	312	3285	1.31%	94%
M-2	726	4291	1.72%	96%
M-3	809	6869	2.75%	87%

#### 4.4. Comparison of three Methods

Finally, the results obtained with the QSI method and with ImageJ were transformed to the 1 to 7 scale used in the CIB W29 templates (see Section 2.2). This enabled the comparison of results among the three methods used, and the goodness of the methodologies used in this work to be checked. In the case of the digital analysis of images, the results of the  $5 \times 5$  filter were shown (the surface pores smaller than  $25 \text{ mm}^2$  were not taken into account in the analysis). With the CIB templates, M-1 and M-2 obtained a value between 3 and 4, and M-3 between 4 and 5. Following the conversion of the results of the method with QSI and ImageJ, the results for M-1 were 3.6 and 3.9; for M-2 it was 3.6 and 3.8, and for M-3 4.5 and 4.6, respectively (Table 3), which supposed that differences went from 2% for M-3, up to 8% for M-1.

The differences obtained after the conversion of values to the scale of 1 to 7 (Table 3) were acceptable for obtaining the results within the CIB W29 range. This could validate the QSI and digital processing methods, and allowed a quick verification of the results. That is, it may be convenient to apply the CIB W29 method together with the others.

**Table 3.** Results of the inspections with the three methods in the scale of 1 to 7.

	QSI	CIB W29	ImageJ
M-1	3.6	3 and 4	3.9
M-2	3.6	3 and 4	3.8
M-3	4.5	4 and 5	4.6

It becomes clear that it is necessary to elaborate a methodology that permits the quantification of the quality of architectural concretes [4]. The QSI method could facilitate the communication between architects, engineers, contractors and concrete manufacturers when seeking to define a surface finish in architectural concrete.

As for the digital method, work should be done to achieve a simple and standardized work protocol to simplify the quality control of the surface finish of concrete elements, including simplifying the inspection from a mobile phone application.

The CIB W29 method it is very intuitive and very rapid to develop, although the inspection lacks objectivity.

## 5. Conclusions

The following conclusions can be drawn from the results of this experimental work:

- (1) Following the conversion of the results of the method with ImageJ and QSI, the results suppose that differences that go from 0.1 tenths (2%) for M-3 up to 0.3 tenths (8%) for M-1. All values are within the obtained range with CIB W29 templates.
- (2) With the digital method, it was shown that 23.5% of the total pores of M-1 have a diameter of less than  $10 \text{ mm}^2$  and 44% of less than  $100 \text{ mm}^2$ . For M-2 and M-3 the proportions of pores with a dimension below  $10 \text{ mm}^2$  is of 43.1% and 27.7%, respectively and that 77.5% and 60.7% are smaller than  $100 \text{ mm}^2$ . From all the above, it can be highlighted that M-1 is the one with the lowest amount of pores; however the proportion of the largest is greater than for M-2 and M-3. In the case of M-3, although it has a lower proportion of larger pores than M-1, its greater amount means that it is the worst in terms of surface finish of the three.
- (3) The simplicity in the application of the method QSI and its ease of implementation in the laboratory or on site was seen. The grouping of pores by diameter does not significantly vary the final results, with similar values to the other two methods being obtained, without extensive knowledge in digital processing. It can be applied on curved surfaces, with different shades or surface spots, without altering the results of the area occupied by the surface pores. The

results obtained, unlike those of the CIB method, quantify the surface affected by the surface pores. The QSI method simplifies work in small areas, but it is not an adequate method for large inspection areas because the identification of surface pores is complicated.

- (4) The CIB W29 method is a good qualitative indicator of the surface quality of concrete elements. It is very intuitive and very rapid to develop, although the inspection lacks objectivity. It does not quantify the area occupied by the pores. The concrete element is only visually compared with a template with different amounts of surface pores.
- (5) The use of image analysis programs allows studying the quality of concrete surface in normal visual conditions. In non-homogeneous zones for changes in tones, shadows, or irregularities, the digital analysis becomes more complex and requires several technical adjustments.

**Acknowledgments:** The authors of this study wish to thank the Department of Architecture and Construction Technology of the Polytechnic University of Cartagena and the Polytechnic University of Valencia.

**Author Contributions:** The results included in this paper were obtained in the PhD thesis carried out by Francisco Benito at Polytechnic University of Valencia (Spain), under the supervision of Manuel Valcuende and Carlos Parra. Francisco Benito wrote the paper. Francisco Benito, Carlos Rodríguez and Isabel Miñano performed the experiments. All the authors contributed to conceive and design the experiments, and to analyses and discuss the results.

**Conflicts of Interest:** The authors declare no conflict of interest.

## References

1. *Tolerances on Blemishes of Concrete, Report Prepared by CIB Working Commission W29, Concrete Surface Finishings*; C.I.B.: Rotterdam, The Netherlands, 1971. Available online: <https://www.irbnet.de/daten/iconda/06059000983.pdf> (accessed on 1 March 2018).
2. Pushpakumara, J.; De Silva, S.; Subashi, G. Visual inspection and non-destructive tests-based rating method for concrete bridges. *Int. J. Struct. Eng.* **2017**, *8*, 74–91. [[CrossRef](#)]
3. Benito, F.; Valcuende, M.; Parra, C.; Rodríguez, C.; Miñano, I. Acabado superficial de hormigones autocompactantes. Método ICS. In Proceedings of the IV Congreso iberoamericano de Autocompactable, Porto, Portugal, 6–7 July 2015.
4. Lemaire, G.; Escadeillas, G.; Ringot, E. Evaluating concrete surfaces using an image analysis process. *Constr. Build. Mater.* **2005**, *19*, 604–611. [[CrossRef](#)]
5. Klovas, A.; Daukšys, M. The influence of form release agent application to the quality of concrete surfaces. *Mater. Sci. Eng.* **2013**, *47*, 012061. [[CrossRef](#)]
6. Tong, X. A new image-based method for concrete bridge bottom crack detection. In Proceedings of the International Conference on Image Analysis and Signal Processing (IASP), Wuhan, China, 21–23 October 2011; pp. 568–571.
7. Chen, Z.Q.; Hutchinson, T.C. Image-Based Framework for Concrete Surface Crack Monitoring and Quantification. *Adv. Civ. Eng.* **2010**, *2010*, 18. [[CrossRef](#)]
8. Majchrowski, R.; Grzelka, M.; Wiczorowski, M.; Sadowski, L.; Gapiński, B. Large Area Concrete Surface Topography Measurements Using Optical 3D Scanner. *Metrol. Meas. Syst.* **2015**, *22*, 565–576. [[CrossRef](#)]
9. Krolczyk, G.M.; Maruda, R.W.; Nieslony, P.; Wiczorowski, M. Surface morphology analysis of duplex stainless steel (DSS) in clean production using the power spectral density. *Measurement* **2016**, *94*, 464–470. [[CrossRef](#)]
10. Nieslony, P.; Krolczyk, G.M.; Zak, K.; Maruda, R.W.; Legutko, S. Comparative assessment of the mechanical and electromagnetic surfaces of explosively clad Ti-steel plates after drilling process. *Precis. Eng.* **2017**, *47*, 104–110. [[CrossRef](#)]
11. Miñano, I.; Benito, F.; Parra, C.; Hidalgo, P. *Concrete Sustainable Light and of High Performance Sustainable. Development and Renovation in Architecture, Urbanism and Engineering*; Springer International Publishing: Cham, Switzerland, 2017; pp. 263–273.
12. Helene, P.R.L.; Alencar, R.; Folch, A.T. Aplicação de concreto auto-adensável na fabricação de pré-moldados. *Técnica* **2008**, *137*, 60–64.

13. Miller, S.A.; Horvath, A.; Ostertag, C.P. Greenhouse gas emissions from concrete can be reduced by using mix proportions, geometric aspects, and age as design factors. *Environ. Res. Lett.* **2015**, *10*, 114017–114028. [[CrossRef](#)]
14. Martínez-Ramírez, S.; Thompson, G.E. Dry and wet “deposition” studies of the degradation of cement mortars. *Mater. Constr.* **1998**, *8*, 15–31. [[CrossRef](#)]
15. Liu, B.; Yang, T. Image analysis for detection of bugholes on concrete surface. *Constr. Build. Mater.* **2017**, *137*, 432–440. [[CrossRef](#)]
16. Rueden, C.T.; Schindelin, J.; Hiner, M.C.; DeZonia, B.E.; Walter, A.E.; Arena, E.T.; Eliceiri, K.W. ImageJ2: ImageJ for the next generation of scientific image data. *BMC Bioinformatics* **2017**. [[CrossRef](#)] [[PubMed](#)]
17. Pacios, A.; González, D.; Escrivá, J.M.; Climent, V. Relationship between SCC Specification and Casting Conditions for Architectural SCC and the Effect on Superficial defects. In Proceedings of the Third North American Conference on the Design and Use of Self-Consolidating Concrete, Chicago, IL, USA, 10–12 November 2008.



© 2018 by the authors. Licensee MDPI, Basel, Switzerland. This article is an open access article distributed under the terms and conditions of the Creative Commons Attribution (CC BY) license (<http://creativecommons.org/licenses/by/4.0/>).